AGU100 ADVANCING EARTH AND SPACE SCIENCE

JGR

Journal of Geophysical Research: Atmospheres

RESEARCH ARTICLE
10.1002/2017JD028064

Key Points:
- Lead-lag analysis and model simulations indicate that the El Niño signal actually leads the stratospheric response by ~2 months
- Considering the time lag, the effects of extreme El Niño on northern polar vortex in late winter are similar with those of moderate events

Correspondence to:
J. Li,
ljp@bnu.edu.cn

Citation:
Zhou, X., Li, J., Xie, F., Chen, Q., Ding, R., Zhang, W., & Li, Y. (2018). Does extreme El Niño have a different effect on the stratosphere in boreal winter than its moderate counterpart? *Journal of Geophysical Research: Atmospheres*, *123*, 3071–3086. https://doi.org/10.1002/2017JD028064

Received 15 NOV 2017
Accepted 5 MAR 2018
Accepted article online 10 MAR 2018
Published online 30 MAR 2018

Does Extreme El Niño Have a Different Effect on the Stratosphere in Boreal Winter Than Its Moderate Counterpart?

Xin Zhou[1,2], Jianping Li[2,3], Fei Xie[2], Quanliang Chen[1], Ruiqiang Ding[1,4], Wenxia Zhang[4], and Yang Li[1]

[1]Plateau Atmosphere and Environment Key Laboratory of Sichuan Province, College of Atmospheric Science, Chengdu University of Information Technology, Chengdu, China, [2]State Key Laboratory of Earth Surface Processes and Resource Ecology and College of Global Change and Earth System Science, Beijing Normal University, Beijing, China, [3]Laboratory for Regional Oceanography and Numerical Modeling, Qingdao National Laboratory for Marine Science and Technology, Qingdao, China, [4]State Key Laboratory of Numerical Modeling for Atmospheric Sciences and Geophysical Fluid Dynamics (LASG), Institute of Atmospheric Physics, Chinese Academy of Sciences, Beijing, China

Abstract A robust impact of El Niño on the Northern Hemisphere (NH) polar stratosphere has been demonstrated by previous studies, although whether this applies to extreme El Niño is uncertain. The time evolution of the response of the NH stratospheric vortex to extreme El Niño, compared with that to moderate eastern Pacific El Niño, is addressed by means of composite analysis using the National Centers for Environmental Prediction/Department of Energy reanalysis data set from 1980 to 2016. Lead-lag analysis indicates that the El Niño signal actually leads the stratospheric response by ~2 months. Considering the time lag, the signal of December-January-February El Niño in the NH stratospheric vortex should mature in the February-March-April season (late winter/early spring). The patterns of circulation and temperature for late winter/early spring during extreme and moderate El Niño events are significant, exhibiting similar structure. The results are confirmed with the Whole Atmosphere Community Climate Model version 4 model, which is forced with observed SSTs of extreme and moderate El Niño in winter (December-January-February) to analyze the day-to-day propagation of their signals. Note that the magnitudes of the stratospheric responses are much larger in the case of extreme El Niño, as stronger upward propagation of planetary waves leads to a weaker northern polar vortex than during moderate El Niño events.

1. Introduction

The El Niño–Southern Oscillation (ENSO), an ocean-atmosphere coupled phenomenon in the tropical Pacific Ocean, is the largest source of tropospheric interannual variability (Bjerknes, 1969; Horel & Wallace, 1981; Trenberth et al., 1998). ENSO has also been found to influence both the tropical and extratropical stratospheric circulation. During the warm ENSO phase (El Niño), enhanced tropical upwelling leads to an upper tropospheric warming and lower stratospheric cooling (Calvo et al., 2004, 2010; Free & Seidel, 2009; Garcia-Herrera et al., 2006; Randel et al., 2009), along with coherent tropical ozone and water vapor variability (Fueglistaler & Haynes, 2005; Geller et al., 2002; Gettelman et al., 2001; Hatsushika & Yamazaki, 2003; Scaife et al., 2003; Xie et al., 2011). Through the deepening of the Aleutian Low in the Pacific North American pattern, El Niño intensifies the vertical propagation of ultralong Rossby waves in the Northern Hemisphere (NH) during winter (e.g., Garcia-Herrera et al., 2006). As waves dissipate at middle-to-high latitudes in the stratosphere, the Brewer-Dobson circulation (Brewer, 1949; Dobson, 1956; Dobson et al., 1929) strengthens, leading to an anomalous warming in the Arctic stratosphere, which has been seen in observational records (Camp & Tung, 2007; Free & Seidel, 2009; Garfinkel & Hartmann, 2007; Labitzke & Loon, 1989; Lan et al., 2012; Ren et al., 2012; Van Loon & Labitzke, 1987; Wei et al., 2007) and reproduced in modeling studies (Garcia-Herrera et al., 2006; Garfinkel, Hurwitz, Oman, & Waugh, 2013; Garfinkel, Hurwitz, Waugh, & Butler, 2013; Hamilton, 1995; Manzini et al., 2006; Rao & Ren, 2015; Sassi et al., 2004; Taguchi & Hartmann, 2006; Xie et al., 2012). The cold ENSO phase (La Niña) has been reported to have a cooling effect on the polar stratosphere (Free & Seidel, 2009; Iza et al., 2016; Mitchell et al., 2011).

In recent decades, ENSO anomaly patterns have changed from their well-known historical forms, motivating a reexamination of the evolution of ENSO events in the tropical Pacific. A new flavor of ENSO, referred to as

the central Pacific (CP) type, has been found to occur with increasing frequency in the tropical Pacific (Ashok et al., 2007; Cai & Cowan, 2009; Kao & Yu, 2009; Kug et al., 2009; Shinoda et al., 2011; Yeh et al., 2009; Zhang et al., 2015); the reasons for this are debated (Ashok et al., 2007; Hu et al., 2016; Kug et al., 2010; Li et al., 2015, 2017; Yeh et al., 2009, 2011). The different spatial patterns of tropical sea surface temperature (SST) anomalies indicate that the climatic impacts of CP El Niño are distinct from those of the traditional, or eastern Pacific (EP), type, both in the troposphere (e.g., Feng & Li, 2011; Weng et al., 2007; Zhang et al., 2011; Zhang et al., 2013, 2014, 2015) and in the stratosphere (Garfinkel, Hurwitz, Oman, & Waugh, 2013; Garfinkel, Hurwitz, Waugh, & Butler, 2013; Hurwitz, Newman, et al., 2011, Hurwitz, Song, et al., 2011; Xie, Li, Tian, Zhang, & Shu, 2014; Xie, Li, Tian, Zhang, & Sun, 2014; Xie et al., 2012). The CP El Niño has been reported to induce a stronger response in the tropical stratosphere than the EP type (Xie, Li, Tian, Zhang, & Sun, 2014), and the two produce opposite effects in the northern polar vortex (Hegyi & Deng, 2011; Iza & Calvo, 2015; Sung et al., 2014; Xie et al., 2012; Zubiaurre & Calvo, 2012). However, apparently contradictory results have also been found, including a weakened northern stratospheric vortex associated with the CP El Niño (Garfinkel, Hurwitz, Oman, & Waugh, 2013; Graf & Zanchettin, 2012; Hurwitz et al., 2014). Garfinkel, Hurwitz, Oman, and Waugh (2013) found that the results are sensitive to the size of the composite and the index used. Iza and Calvo (2015) further clarified that a robust signal of CP El Niño, which is distinguishable from that of EP type, is found when only winters without sudden stratospheric warming are considered.

Recently, extreme El Niño has been projected to occur with higher frequency in the future due to global warming (Cai et al., 2014; Wang et al., 2017). Three unusually strong extreme El Niño events in the satellite era, the 1982/1983 extreme El Niño (Philander, 1983), the 1997/1998 El Niño (often referred to as "the climate event of the twentieth century") (Changnon, 2000; McPhaden, 1999), and the strongest El Niño in history, which developed in the eastern Pacific during the winter of 2015/2016 (Levine & McPhaden, 2016), were each characterized by an exceptional warming, with the area in which SSTs exceeded 28°C extending into the eastern equatorial Pacific. These extreme El Niño events have already severely affected global weather patterns, resulting in major natural disasters and subsequent socioeconomic stress (e.g., Cai et al., 2014; Geng et al., 2017; McPhaden et al., 2006). Extreme El Niño events involve not simply a strengthening of moderate El Niño patterns but also a considerable eastward shift of the tropical convection (Rao & Ren, 2016a, 2016b; Xu et al., 2016), leading to a nonlinear and asymmetric Pacific North American wave train pattern in the extratropics (Rao & Ren, 2016a, 2016b). However, whether extreme El Niño has distinct effects on the stratosphere is still highly uncertain and is the subject of much research. Some recent studies have focused on the stratospheric impacts of extreme El Niño. Rao and Ren (2016a, 2016b) noted the nonlinearity of the impact on the northern winter stratosphere of ENSO events of different intensity, and Rao and Ren (2017) reported that the three extreme El Niño events had a major impact on stratospheric circulation based on observations. Richter et al. (2015) found a more linear stratospheric response to El Niño in simulations, with strong amplitude in the case of extreme El Niño (the 1982/1983 and 1997/1998 events in their study). Unprecedented variations in the stratosphere caused by extreme El Niño events, such as in the quasi-biennial oscillation (QBO) and water vapor, have been observed (Avery et al., 2017; Christiansen et al., 2016; Dunkerton, 2016; Garfinkel et al., 2017; Varotsos et al., 2017).

Palmeiro et al. (2017) found that the 2015/2016 El Niño led to a stronger northern polar vortex in winter, which is not consistent with the well-known result that El Niño events can warm and weaken the northern polar vortex. However, whether extreme El Niño events have opposite high-latitude stratospheric impacts to those of moderate El Niño events still deserves further investigation. It is well known that vortex variability occurs even without any changes in tropospheric state. That means part of variations of the stratospheric polar vortex is possibly unforced and has nothing to do with El Niño, which happens to be occurring simultaneously. Idealized models of vortex variability in some cases exhibit bifurcations in their behavior that are extremely sensitive to initial conditions and external parameters (Matthewman & Esler, 2011; Yoden, 1987). This would imply that vortex variability on monthly and seasonal time scales is extremely difficult to predict, at least in a deterministic sense. Evidence for such bifurcations in forecast models has been found (Noguchi et al., 2016). Although El Niño can help enhance stratospheric predictability in a statistical sense (Domeisen et al., 2015; Sigmond et al., 2013), anomalies of stratospheric vortex cannot be assumed to be forced by that winter El Niño (Garfinkel, Hurwitz, Oman, & Waugh, 2013).

Table 1
Extreme and Moderate Events in Observations Studied Separately and as Composites

Composite	Years
Extreme El Niño	1982/1983, 1997/1998, 2015/2016
Moderate El Niño	1986/1987, 1987/1988, 2006/2007

Motivated by this, our study aims to understand the stratospheric response to extreme El Niño events not only by means of observation analysis but also using time-slice experiments with Whole Atmosphere Community Climate Model version 4 (WACCM4), compared with that of moderate El Niño events. The remainder of this paper is organized as follows. Section 2 presents the data, model, and analysis methods used. In section 3, we document the observational signal of extreme El Niño events in stratospheric temperature and circulation in boreal winter (December-January-February; DJF) and also in late winter/early spring (February-March-April; FMA), and then discuss the physical connections. Model simulations to confirm these results are shown in section 4. Finally, we summarize the main findings in section 5.

2. Data and Methodology

2.1. Extreme and Moderate El Niño

El Niño events are identified when SST anomalies in the Niño3.4 region exceed 0.5°C (Trenberth & Stepaniak, 2001), based on the DJF seasonal mean SST anomalies in the Hadley Centre Sea Ice and Sea Surface Temperature (HadISST) data set (Rayner et al., 2003) relative to a 1981–2010 base period. To avoid possible confusion with CP El Niño events, we did not include CP events in our study. Here we used the Cold Tongue and Warm Pool indices (Ren & Jin, 2011) to identify EP and CP events, respectively, and CP El Niño events are excluded in our study. The 1982/1983, 1997/1998, and 2015/2016 events were exceptionally strong, measured either by the zonal contrast in SST anomalies (Giese & Ray, 2011; Kao & Yu, 2009; Kug et al., 2009; Larkin & Harrison, 2005a, 2005b) or using variables other than SST (Chiodi & Harrison, 2010; Singh et al., 2011). These three events, by the Niño3.4 measure here (L'Heureux et al., 2017), fall into the "extreme" category in our study, while other EP events are identified as "moderate" El Niño events. The years included in each composite are listed in Table 1. Composite winter SST anomaly patterns for extreme and moderate El Niño are shown in Figures 1a and 1b, respectively. Although they exhibit similar EP patterns, it is apparent that extreme El Niño is much stronger than moderate El Niño and features larger SST anomalies. The SST anomalies for the three extreme El Niño events are shown separately in Figures 1c–1e. In winter, all these events had developed to their mature stage. Most of the events peaked in late fall or early winter and decayed by the following spring. Therefore, for brevity and to maximize the signal, in the following analysis we consider boreal winter (DJF) as the reference period for El Niño events.

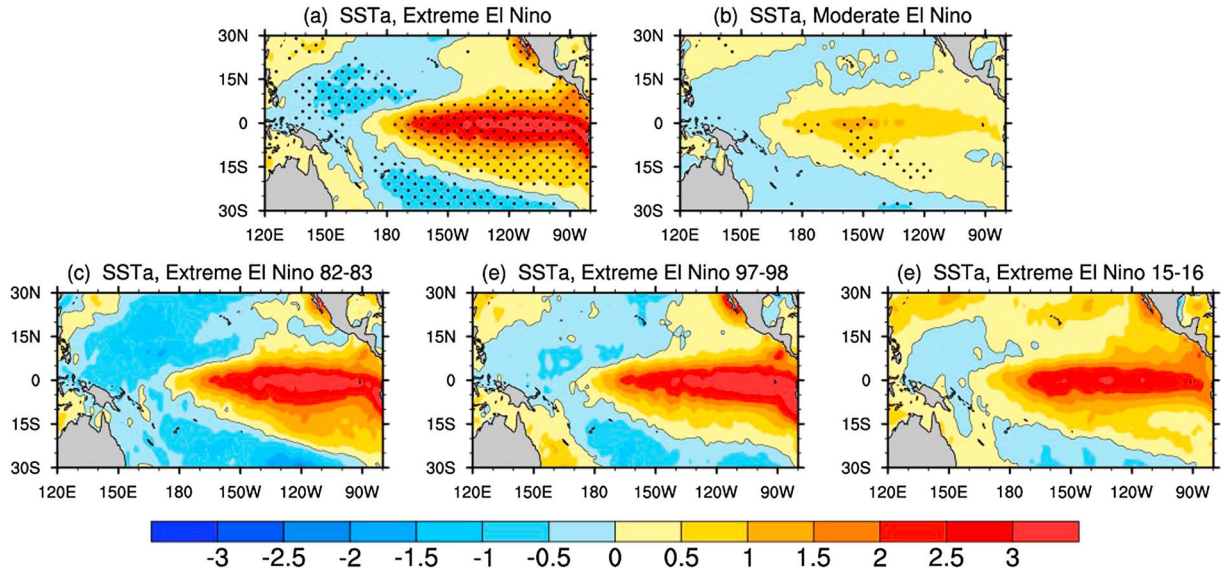

Figure 1. Composite winter (December-January-February) sea surface temperature (SST) anomalies (°C) for (a) extreme El Niño events and (b) moderate El Niño events, from Hadley Centre Sea Ice and Sea Surface Temperature. Also shown are winter SST anomalies (°C) for three extreme El Niño events: (c) 1982/1983, (d) 1997/1998, and (e) 2015/2016. Contours are drawn at ±0.5°C. Anomalies that are significant at the 90% confidence level (Student's *t* test) are stippled.

Table 2
Description of the WACCM4 Experiments

Experiment	Details
R1	R1: control run using CESM case F_2000_WACCM_SC. Prescribed SST forcing of the monthly mean climatology from 1980 to 2015.
R2	R2: as for R1, but with extreme El Niño SST forcing prescribed in the tropical Pacific (30°S–30°N, 120–280°E). The forcing is limited to December–February and is set to 0 for the rest of the year.
R3	R3: as for R1, but with moderate El Niño SST anomalies added in the tropical Pacific (30°S–30°N, 120–280°E). The forcing is limited to December–February and is set to 0 for the rest of the year.

Note. WACCM4 = Whole Atmosphere Community Climate Model version 4; CESM = Community Earth System Model; SST = sea surface temperature.

2.2. Observational Data

The selected El Niño events are studied via composite analysis and case studies in boreal winter using two data sets. SST data were taken from the HadISST data set (Rayner et al., 2003), with a horizontal resolution of 1° × 1°, while monthly mean wind, temperature, and geopotential height data for the period 1980–2016 were taken from the National Centers for Environmental Prediction/Department of Energy (NCEPDOE) reanalysis, on 17 pressure levels from 1,000 to 10 hPa, on a 2.5° × 2.5° horizontal grid. To verify the NCEPDOE results, data from the European Centre for Medium Range Weather Forecasts reanalysis, ERA-Interim, were also used (Simmons, Uppala, & Dee, 2007, Simmons, Uppala, Dee, & Kobayashi, 2007; Uppala et al., 2008). The main results from these two reanalysis data sets are in close agreement, and so only the results from NCEPDOE reanalysis are presented here. The Niño3.4 index and Niño3 index used in this study are available at the Climate Prediction Center (http://www.cpc.noaa.gov/data/indices/). The 10.7 cm solar radio flux, or $F_{10.7}$, is used as the index of solar activity (ftp://ftp.ngdc.noaa.gov/STP/space-weather/solar-data/solar-features/).

2.3. Model

The WACCM is a state-of-the-art chemistry climate model developed at the National Center for Atmospheric Research and can be used as the atmospheric component of the Community Earth System Model (Hurrell et al., 2013). The version used in our experiments, WACCM4, has a horizontal resolution of 1.9° × 2.5° and does not include interactive chemistry (Garcia et al., 2007). The vertical resolution is 1.1–1.4 km in the tropical tropopause layer and the lower stratosphere (height below 30 km), with 66 vertical levels extending from the ground to 4.5×10^{-6} hPa (~145 km geometric altitude). Garcia et al. (2007) and Marsh et al. (2013) provide a complete description of the model, and the latest modifications to the chemistry module and to the orogravity wave drag scheme can be found in Solomon et al. (2015). Fixed greenhouse gas values, averages over the period 1980–2015 from emissions scenario A2 of the Intergovernmental Panel on Climate Change (WMO, 2003), were used in the model's radiation scheme. The prescribed ozone forcing used in our experiments is a 12 month seasonal cycle taken from Coupled Model Intercomparison Project Phase 5 ensemble mean ozone output averaged over the period 1980–2015. QBO phase signals with a 28 month fixed cycle (nudged QBO) were included in WACCM4 as an external forcing for zonal wind.

Three experiments with daily outputs, designed to analyze day-to-day propagation of the El Niño signal, are described in this paper. All experiments were conducted using the same prescribed greenhouse gas but with different SST forcings. The control run, R1, used a monthly mean SST climatology from the period 1980–2015; experiment R2 used the same SST as the control run but with extreme El Niño SST forcing prescribed in the tropical Pacific (30°S–30°N, 120–280°E) over a limited period; and R3 used the same SST as the control run but with moderate El Niño SST forcing prescribed in the tropical Pacific (30°S–30°N, 120–280°E). The forcing is limited to December to February and is set to 0 over the rest of the year. Prescribed SSTs are obtained from composite anomalies from extreme El Niño and moderate El Niño events (Table 1) from December to February. A summary of all the experiments is given in Table 2. The experiments were each run for 33 years, with the first 3 years excluded as spin-up. The remaining 30 years were used for the analysis, and model climatologies were obtained from this period.

The key point of the experiments is to isolate the signal of extreme and moderate El Niño in winter, so that the stratospheric responses in winter and late winter/early spring are attributed to the winter El Niño forcing.

2.4. Analysis Methods

Monthly anomalies are calculated by subtracting the long-term mean of each calendar month from each individual month. The linear trends have been removed using regression analysis from the temperature and zonal wind data before analysis. To avoid possible interference from the QBO, we filtered out the biennial circulation anomalies (24–32 months) from temperature and circulation fields between 100 and 10 hPa. Matthes et al. (2004), Labitzke, Kunzel, and Bronnimann (2006), Camp and Tung (2007), and others have found a significant impact of the solar cycle on the polar vortex, so the solar cycle signal is also removed based on linear regression using the $F_{10.7}$ index. Composite analysis and lead-lag correlation methods are applied to the stratospheric response during El Niño events. Because of the limited number of events involved in our composite analysis, the significance of composite results is determined by establishing whether the variations of each event are in the same phase (e.g., Schar et al., 2016). That is, if the anomalies of all the events agree on the sign of change, then it is significant. The statistical significance of the correlation between two autocorrelated time series is determined from a two-tailed Student's *t* test using the effective number of degrees of freedom (Li et al., 2013; Pyper & Peterman, 1998; Xie, Li, Tian, Zhang, & Shu, 2014), as given by the following approximation:

$$\frac{1}{N^{\mathrm{eff}}} \approx \frac{1}{N} + \frac{2}{N}\sum_{j=1}^{N}\frac{N-j}{N}\rho_{XX}(\mathrm{j})\rho_{YY}(\mathrm{j}).$$

where N is the sample size and $\rho_{XX}(\mathrm{j})$ and $\rho_{YY}(\mathrm{j})$ are the autocorrelations of two sampled time series X and Y at time lag j, respectively.

Two indices are used as representative measures of the strength of the stratospheric temperature and circulation response:

1. *Stratospheric polar cap temperature (SPT)*. SPTs are temperature anomalies averaged over the polar cap north of 60°N, between 100 and 10 hPa. This is used as a measure of stratospheric warming.
2. *Geopotential height index (GHI)*. GHI is the difference between geopotential height anomalies averaged over the zonal belts 30°–50°N and 70°–90°N, between 100 and 10 hPa. GHI measures the strength of the meridional gradient of geopotential height and is an indication of changes in zonal wind around 60°N.

Wave activity analysis was used to investigate stationary Rossby wave energy propagation (Edmon et al., 1980; Hu & Tung, 2002; Mukougawa & Hirooka, 2004; Randel, 1987). The wave activity flux is directed parallel to the group velocity of stationary Rossby waves, making it a useful indicator of the propagation direction and source of stationary atmospheric Rossby waves. Following Chen et al. (2003) and Rao and Ren (2015), daily data are used to calculate the Eliassen-Palm (E-P) flux. The formulae to calculate the quasi-geostrophic 2-D E-P flux were given by Andrews et al. (1987). The meridional (F_y) and vertical (F_z) components of the E-P flux and the E-P flux divergence D_F are calculated as follows:

$$F_y = -\rho_0 a\cos\varphi\overline{u'v'},$$

$$F_z = -\rho_0 a\cos\varphi\frac{Rf}{HN^2}v'T'$$

$$D_F == \frac{\nabla\cdot F}{\rho_0 a\cos\varphi} = \frac{\partial\left(F_y\cos\varphi\right)/(a\cos\varphi)\partial\varphi + \partial F_z/\partial z}{\rho_0 a\cos\varphi},$$

where ρ_0 is air density, a is the radius of the Earth, R is the gas constant, f is the Coriolis parameter, H is the atmospheric scale height (7 km), u and v are the zonal and meridional wind components, respectively, z and φ are the height and latitude, respectively, and T is the temperature; overbars denote zonal means, and prime symbols denote departures from the zonal mean.

3. Impact of Extreme El Niño on the Winter Stratosphere

Many studies have focused on the winter mean response of NH stratospheric polar vortex to El Niño. However, the importance of studying the time evolution of the El Niño response from early to late winter/early spring has already been emphasized and is essential for depicting the coupling between the stratosphere and troposphere (e.g., Calvo et al., 2017; Fletcher & Kushner, 2011; Ineson & Scaife, 2009; Manzini et al., 2006; Sung et al., 2014). Particularly, Manzini et al. (2006) reported a polar warming

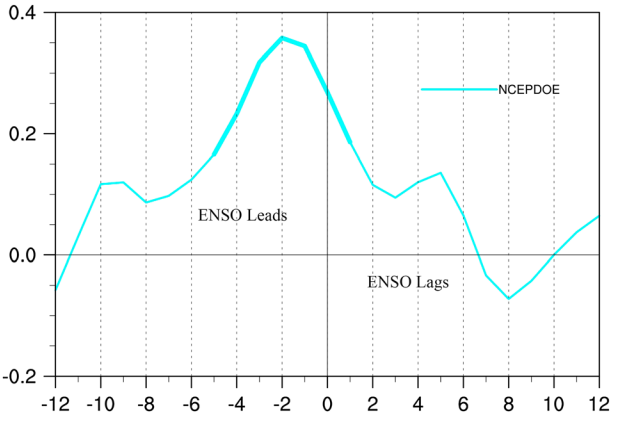

Figure 2. Lead-lag correlation between the 3 month averaged stratospheric polar cap temperature (60°N–90°N) anomalies and the winter (December-January-February averaged) Niño3.4 index for the period 1980–2016, from the National Centers for Environmental Prediction/Department of Energy (NCEPDOE) reanalysis data set. Negative (positive) lags indicate that El Niño–Southern Oscillation (ENSO) is leading (lagging), and thicker lines indicate statistical significance at the 95% confidence level.

occurring in late winter/early spring due to El Niño. Previous studies have also found that it takes a few months for the stratosphere to establish a stable pattern of response to tropical SST anomalies (Calvo et al., 2004, 2010; Garcia-Herrera et al., 2006; Jin & Hoskins, 1995; Newman et al., 2001; Yulaeva & Wallace, 1994). We investigate the lead-lag correlation between the monthly NH SPT (a measure of stratospheric warming; see section 2.4) and the winter (DJF averaged) Niño3.4 index (Figure 2). The maximum correlation coefficients (significant at the 95% confidence level) occur at a lag of 2 months (ENSO leading SPT); the simultaneous correlation coefficient is smaller. This suggests that the response of NH high-latitude stratospheric temperature to El Niño lags behind the El Niño events. Note also that the maximum correlation coefficient in Figure 2 is ~0.4, which indicates that most of the vortex variability in DJF is not explained by ENSO, supporting the view developed by Garfinkel, Hurwitz, Oman, and Waugh (2013). Therefore, the following sections present the composite NH stratospheric circulation and temperature anomalies during winter (DJF) and late winter/early spring (FMA).

3.1. Winter (DJF) Seasonal Mean

Composite analysis is performed to investigate the impact of extreme El Niño events on the stratosphere in boreal winter (DJF), compared with that of moderate EP El Niño events (Figure 3; see section 2 for identification methods). In the tropical stratosphere, out-of-phase temperature variations (cooling) in the middle stratosphere and in-phase variations (warming) in the tropical lower stratosphere are found during extreme El Niño events, with larger amplitudes than those during moderate events. The intense tropical variations during extreme El Niño are consistent with previous studies (Rao & Ren, 2016a, 2016b; Xu et al., 2016) and can be accounted for by the traditional paradigm (Calvo et al., 2010; Free & Seidel, 2009; Hardiman et al., 2007; Randel, 1987). Interestingly, the composite pattern of the stratospheric polar vortex in the NH high latitudes is cooled and strengthened. It seems to be opposite to the traditional pattern, but it should be noted that the pattern is not significant. Caution must be applied when the events involved in composite analysis are limited (Garfinkel, Hurwitz, Oman, & Waugh, 2013). In Figure 4, we present the

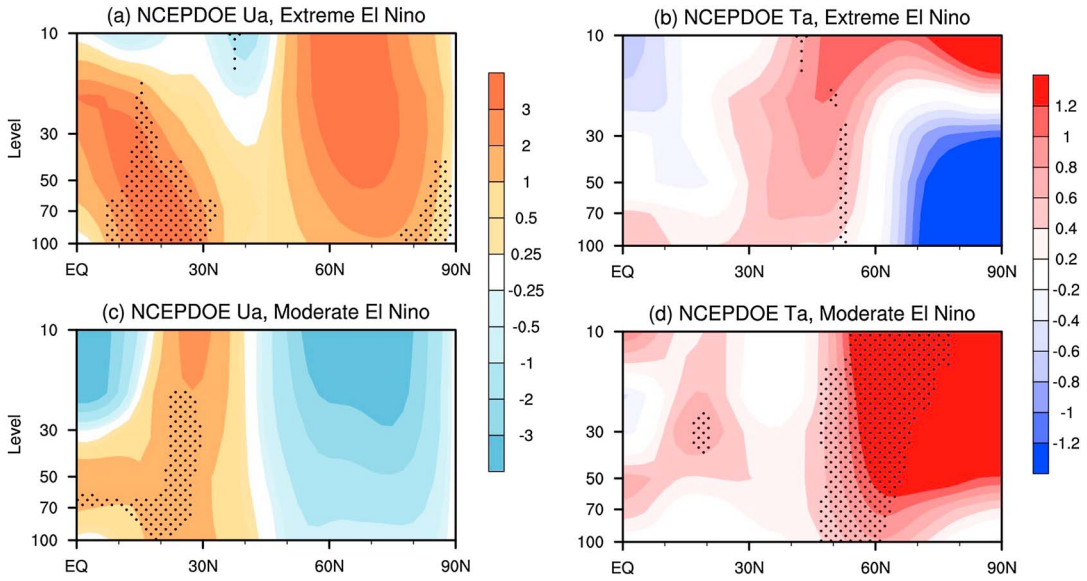

Figure 3. Composite zonal wind (a, c; units: m s^{-1}) and temperature (b, d; units: K) anomalies for (a, b) extreme El Niño and (c, d) moderate El Niño in winter (December-January-February), from the National Centers for Environmental Prediction/Department of Energy (NCEPDOE) reanalysis. The annual cycle, linear trend, and quasi-biennial oscillation signals have been removed from the temperature and zonal wind data. Stippling denotes that anomalies are significant; that is, the sign of the change is the same for all events.

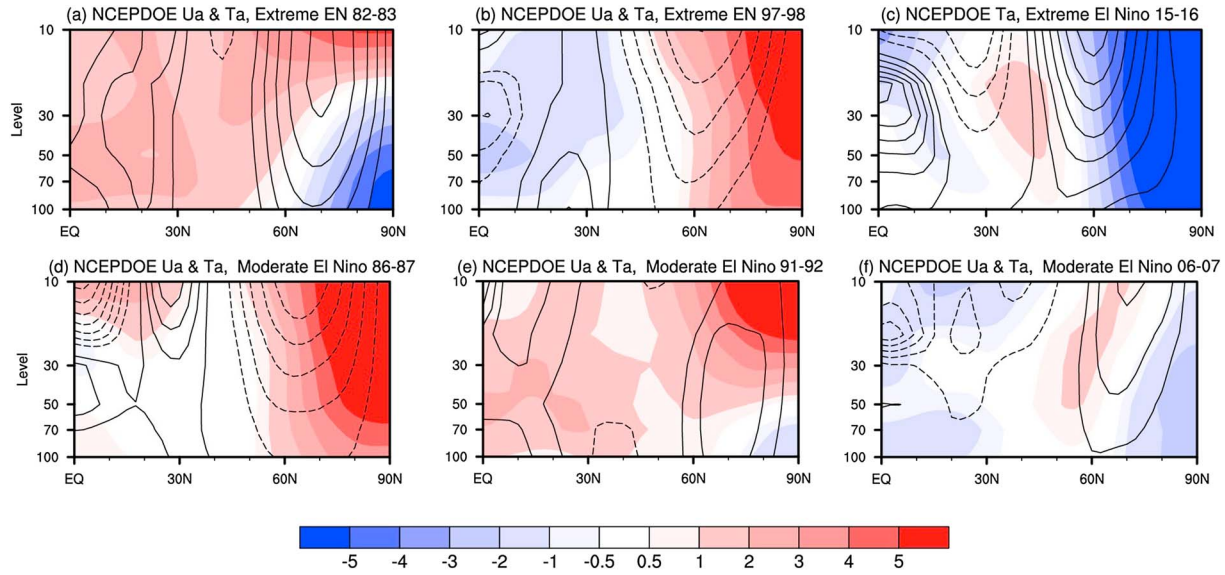

Figure 4. Zonal wind (contours; units: m s^{-1}) and temperature (shading; units: K) anomalies in winter (December-January-February) from the National Centers for Environmental Prediction/Department of Energy (NCEPDOE) reanalysis for each of the (a–c) three extreme El Niño (EN) events and (d–f) three moderate El Niño events.

zonal-mean zonal wind and temperature anomalies in winter (DJF) for all selected extreme and moderate events, from the NCEPDOE reanalysis. Features apparently at odds with the averaged anomaly patterns obtained in the composite analysis are seen in individual cases within the moderate group, including the 1997/1998 and 2006/2007 El Niño events. They lead to the insignificant composite anomalies in Figure 3.

El Niño perturbs the polar stratospheric circulation by altering the propagation and dissipation of ultralong-wavelength Rossby waves in middle latitudes (Cagnazzo et al., 2009; Free & Seidel, 2009; Garcia et al., 2007; Garcia-Herrera et al., 2006; Garfinkel & Hartmann, 2008; Hamilton, 1993; Manzini et al., 2006; Sassi et al., 2004; Taguchi & Hartmann, 2006; Van Loon et al., 1982). Therefore, we investigate the winter planetary wave activity during each El Niño event. Given the lagged response of polar stratospheric anomalies to upward wave activity (Newman et al., 2001), we focus on the November-December mean planetary wave activity. Figure 5 shows the latitude-height structure of the E-P flux anomalies in the six El Niño events. Reduced upward wave activity during early winter of 1982/1983 and 2015/2016 (Figures 5a and 5c) corresponds to

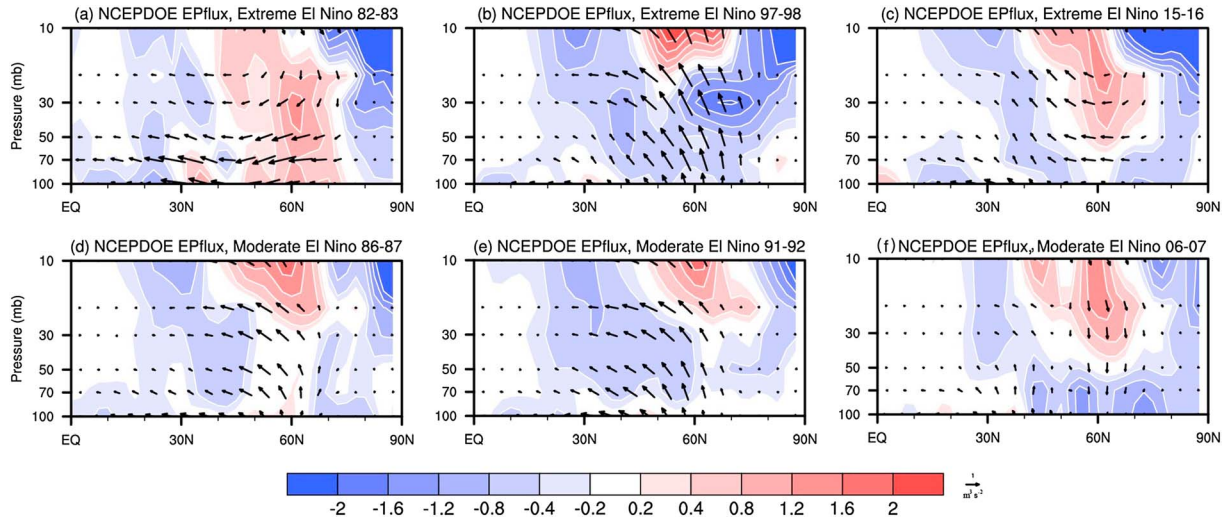

Figure 5. November to December Eliassen-Palm (E-P) flux response (vectors, normalized by air density; units: 10^7 m^3 s^{-2}) and E-P flux divergence (color shading, units: m s^{-1} day^{-1}) from the National Centers for Environmental Prediction/Department of Energy (NCEPDOE) reanalysis for each of the (a–c) three extreme El Niño events and (d–f) three moderate El Niño events.

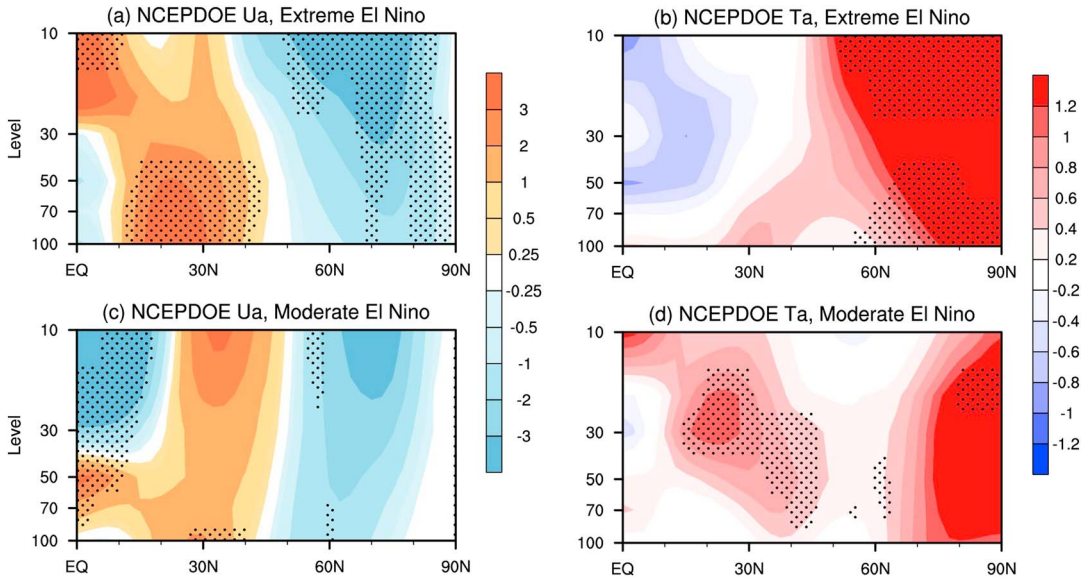

Figure 6. Late winter/early spring (February-March-April) composite zonal wind (a, c; units: m s^{-1}) and temperature (b, d; units: °C) anomalies from the National Centers for Environmental Prediction/Department of Energy (NCEPDOE) reanalysis for (a, b) extreme El Niño and (c, d) moderate El Niño. Stippling denotes anomalies where all events have the same sign.

the observed colder and stronger polar vortex (Figures 4a and 4c). Palmeiro et al. (2017) found that anomalous Rossby waves interfered destructively with the climatological stationary wave in November and December 2015 (their Figure 3). This result is consistent with the wave activity diagnosed here during the early winter of 2015/2016. Although the 1982/1983 extreme El Niño exhibits similarly weakened upward wave activity, increased upward wave activity is found in early winter in 1997/1998 (Figure 5b), leading to the weakened polar vortex (Figure 4). Rao and Ren (2017) provided insight into possible causes leading to different NH stratospheric variations in winter during these three extreme El Niño events. In addition, during the 2006/2007 moderate El Niño in early winter, upward wave activity at high latitudes is reduced, unlike that in other moderate El Niño events. This accounts for the cooled polar vortex during winter 2006/2007 (Figure 4f).

3.2. Late Winter/Early Spring (FMA) Seasonal Mean

Although the composite polar vortex anomalies during extreme and moderate El Niño events seem to be antisymmetric, more careful analysis of individual El Niño events casts doubt on this result. It is difficult to obtain a robust averaged pattern in boreal winter for either extreme or moderate El Niño due to the confounding effects of internal unforced variability. The lead-lag response analysis suggests that the most pronounced response of NH high-latitude stratospheric temperature to El Niño should occur in late winter/early spring.

Figure 6 shows the late winter/early spring (FMA averaged) composite anomalies of zonal-mean zonal wind and temperature for extreme and moderate El Niño events from the NCEPDOE reanalysis. Contrary to the composite results in Figure 3, the northern polar vortex variations in late winter/early spring during extreme El Niño and moderate El Niño are similar, exhibiting a weakened and warm northern polar vortex. The circulation and temperature anomalies in late winter/early spring are in good agreement with previously established El Niño signatures (Cagnazzo et al., 2009; Free & Seidel, 2009; Garcia-Herrera et al., 2006; Xie et al., 2012). Moreover, the circumpolar zonal wind and temperature anomalies during extreme El Niño events are stronger and extend farther into the midlatitudes than those during moderate El Niño events.

To further confirm the similarity between the extreme and moderate El Niño patterns in late winter/early spring, the circulation and temperature anomalies in late winter/early spring (FMA) for the six El Niño events are shown separately in Figure 7. Easterly anomalies and anomalous warming are clearly seen in the northern polar region during all extreme and moderate El Niño events. In addition, with larger zonal wind and

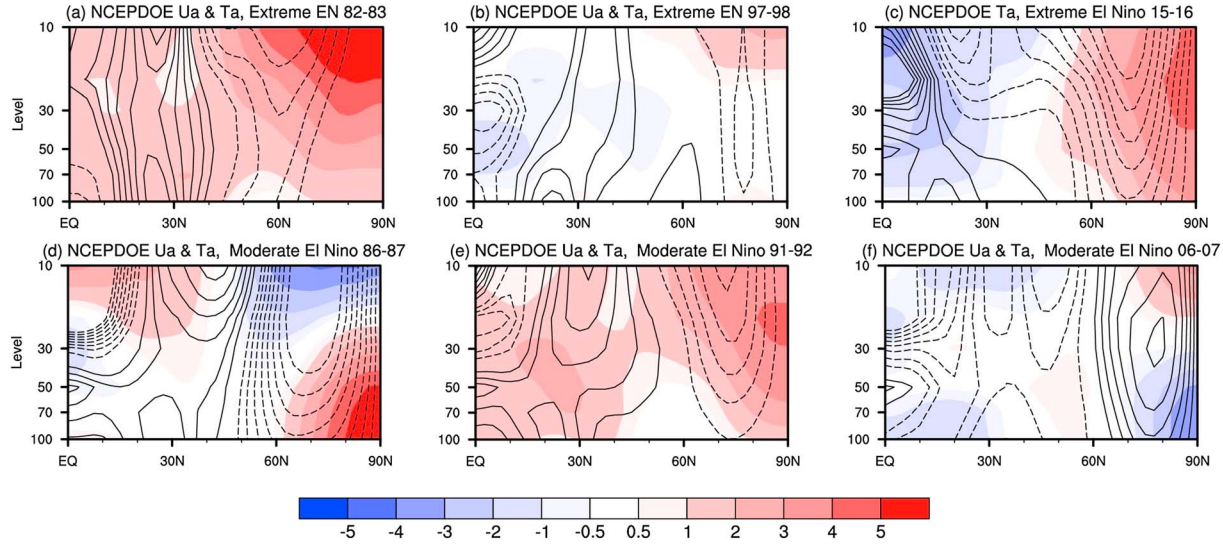

Figure 7. As for Figure 4, but in late winter/early spring (February-March-April).

temperature anomalies, extreme El Niño seems to have a stronger effect on the polar vortex than moderate El Niño, which is consistent with the late-winter composite analysis (Figure 6).

The late winter/early spring planetary wave activity during each El Niño event is also diagnosed. Figure 8 shows the latitude-height structure of the E-P flux anomalies in the six El Niño events during January and February. Note that the January-February mean of planetary wave activity is investigated because of the lagged response of polar stratospheric anomalies to upward wave activity. Anomalous wave flux enters the stratosphere at ~60° latitude in the NH in late winter/early spring; this effect can be observed during all events. As a result, the northern polar vortex becomes warmer and weaker in late winter/early spring during both extreme and moderate El Niño (Figures 6 and 7).

Finally, the temporal evolution of the polar temperature and midlatitude jet response from winter to the following spring is presented in Figure 9. Here we use vertical time sections of indices, SPT and GHI, which are described in section 2. In both the extreme and moderate El Niño case, a warming of the polar atmosphere, indicated by the negative anomalies of SPT, is in agreement with the signal in zonal mean temperature (Figures 3 and 6); so is a deceleration of the midlatitude jet revealed by the negative anomalies of GHI. It is clearly shown that a maximum response is established during February to March for both extreme and moderate El Niño, supporting the lagged response obtained using the lead-lag analysis. In addition, the

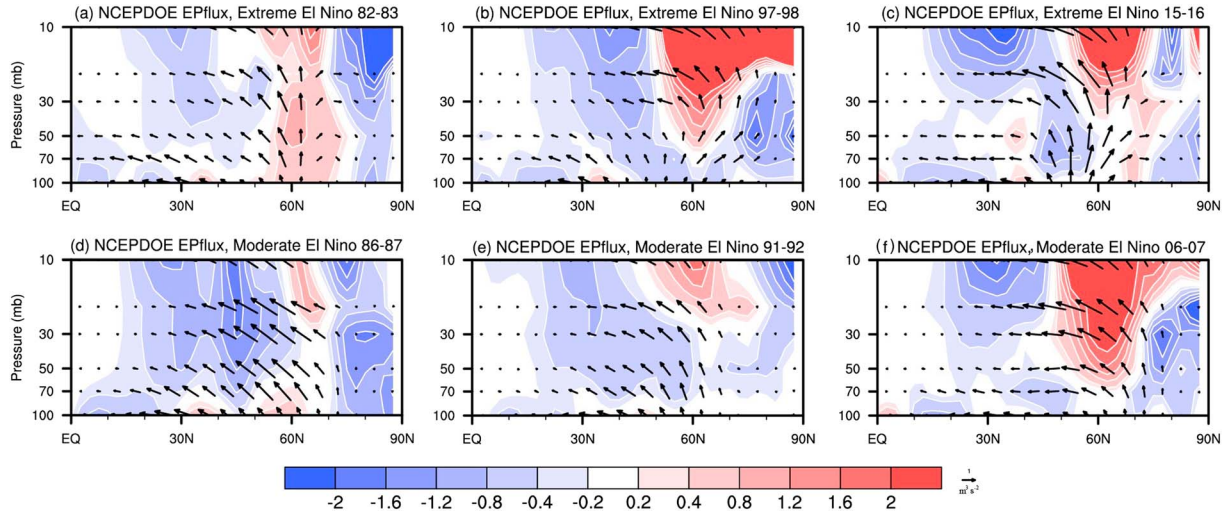

Figure 8. As for Figure 5, but from January to February.

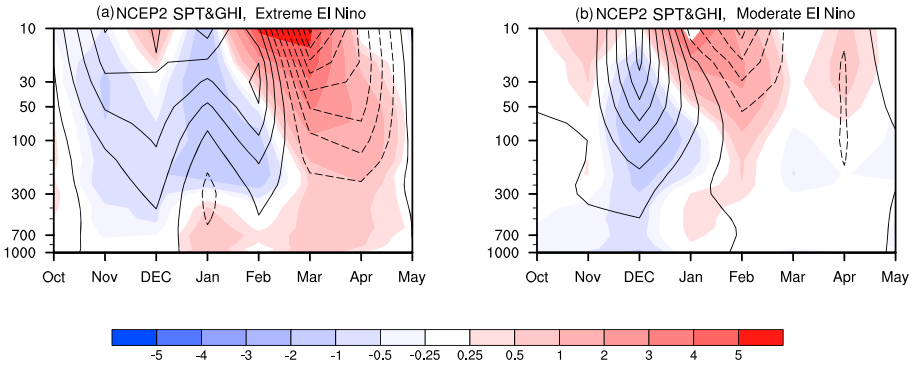

Figure 9. Pressure-time cross sections of geopotential height index (GHI; contours; interval: 50 m) and stratospheric polar cap temperature (SPT; shading; units: K) for (a) extreme El Niño composites and (b) moderate El Niño composites.

variations in the NH polar vortex have much larger amplitude in the case of extreme El Niño than that of moderate El Niño. This feature is also coherent with the seasonal mean results above.

4. Model Simulations With WACCM4

Due to the limited number of EP El Niño events that have occurred in recent decades and the large internal climate variability, it is necessary to supplement the signature of extreme El Niño events obtained from reanalyses. We used WACCM4 to perform a series of idealized numerical experiments to confirm our results (section 2.3). Figure 10 shows vertical cross sections of SPT and GHI for extreme and moderate El Niño events, based on WACCM4 simulations forced by SST anomalies of extreme and moderate El Niño limited to winter (DJF). The polar cap temperature response during extreme El Niño is of greater amplitude than that during moderate El Niño (Figure 10). Consistently, there is a stronger (more than twice as strong) significant negative GHI response, indicating a weakening stratospheric jet, in extreme El Niño than in moderate El Niño. The common feature of both extreme and moderate El Niños, however, is the lagged response starting from February and lasting until April. This feature is more clearly shown in the case of moderate El Niño, when the warmed polar vortex and weakened stratospheric jet appear from 1 February. Although in extreme El Niños a

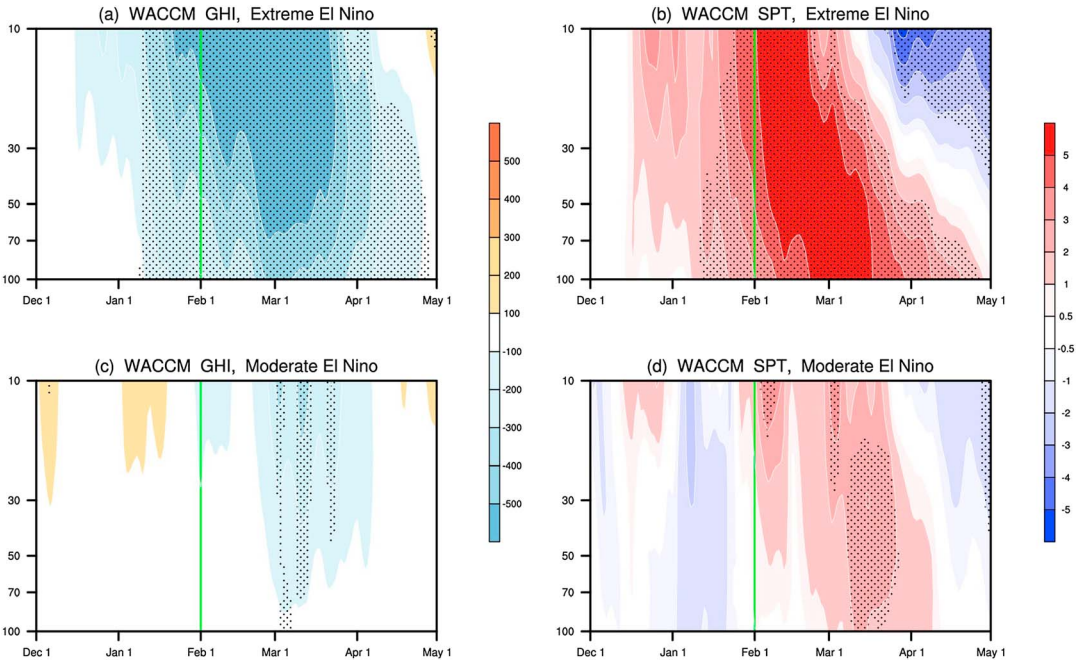

Figure 10. Height-time cross sections of geopotential index (GHI: a, c; units: m) and stratospheric polar cap temperature (SPT: b, d; units: K) for (a, b) extreme El Niño and (c, d) moderate El Niño, based on Whole Atmosphere Community Climate Model version 4 (WACCM4) simulations. Anomalies that are significant at the 90% confidence level (Student's *t* test) are stippled.

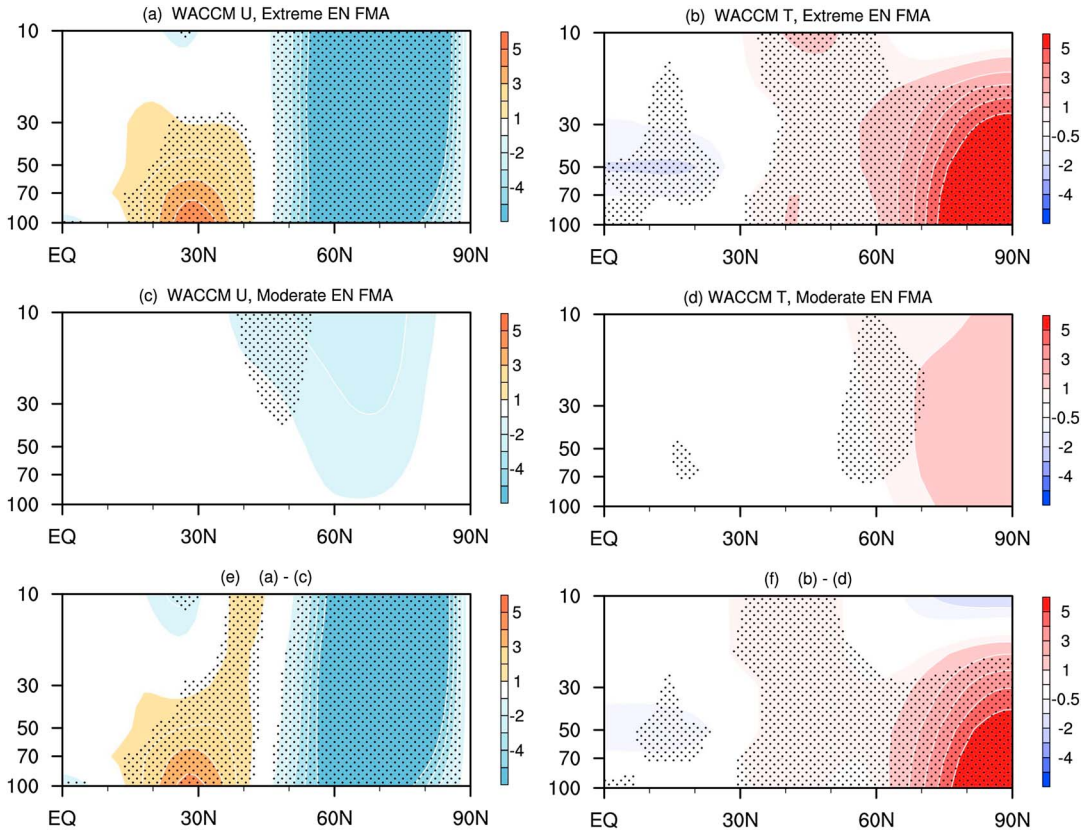

Figure 11. Zonal-mean zonal wind (a, c, e; units: m s^{-1}) and temperature (b, d, f; units: K) anomalies for (a, b) extreme El Niño (EN) and (c, d) moderate El Niño in late winter/early spring (February-March-April) from Whole Atmosphere Community Climate Model version 4 (WACCM4) simulations. (e, f) Differences between extreme and moderate El Niño for zonal wind and temperature, respectively. Anomalies that are significant at the 90% confidence level (Student's *t* test) are stippled.

substantial warming of the polar stratosphere starts 2 weeks after the forcing begins (December), it gradually increases and significant anomalies are established after 1 February. Therefore, apart from a stronger stratospheric response to extreme El Niño than to moderate El Niño, a time lag of about 2 months is revealed by the simulations. This supports the lead-lag analysis using observations, as presented in section 3 (Figure 2). The lagged response indicates that the late winter/early spring variations in the NH stratosphere during El Niño events may better represent the impact of El Niño at high latitudes.

The zonal mean temperature and zonal wind anomalies during late winter/early spring (FMA) are presented in Figure 11. A significantly warmed polar vortex and weakened circumpolar jet are found in both extreme and moderate El Niño cases. The signatures of extreme and moderate El Niño have a similar pattern, but extreme El Niño has significantly larger amplitudes. The nonlinearity of the impact on the northern winter stratosphere of ENSO events of different intensity has been discussed in previous studies (Rao & Ren, 2016a, 2016b), but in our experiments the amplitude of the NH stratospheric response to extreme El Niño is 4 times larger than that to moderate El Niño. This discrepancy presumably arises from different aspects focused on in the two studies. More discussion is presented in section 5. Note also that the model results do not agree with observations for early winter. In reality, the most vortex variability is not explained by ENSO. This view has been developed by Garfinkel, Hurwitz, Oman, and Waugh (2013) and is also supported by our lead-lag analysis (Figure 2). However, the sensitive runs in WACCM4 isolate the ENSO signal. Therefore, it is not particularly surprising that differences exist between observations and simulations. On the other hand, previous studies and the lead-lag analysis as well as model simulations in our study have shown that the response of the stratospheric polar vortex to El Niño matures in late winter/early spring. Therefore, significant signals of El Niño are found in late winter/early spring, which are coherent with model simulations.

The physical connection between El Niño and the stratosphere is further confirmed here from model simulations. Figure 12 shows the monthly evolution of planetary wave activity in the NH from December

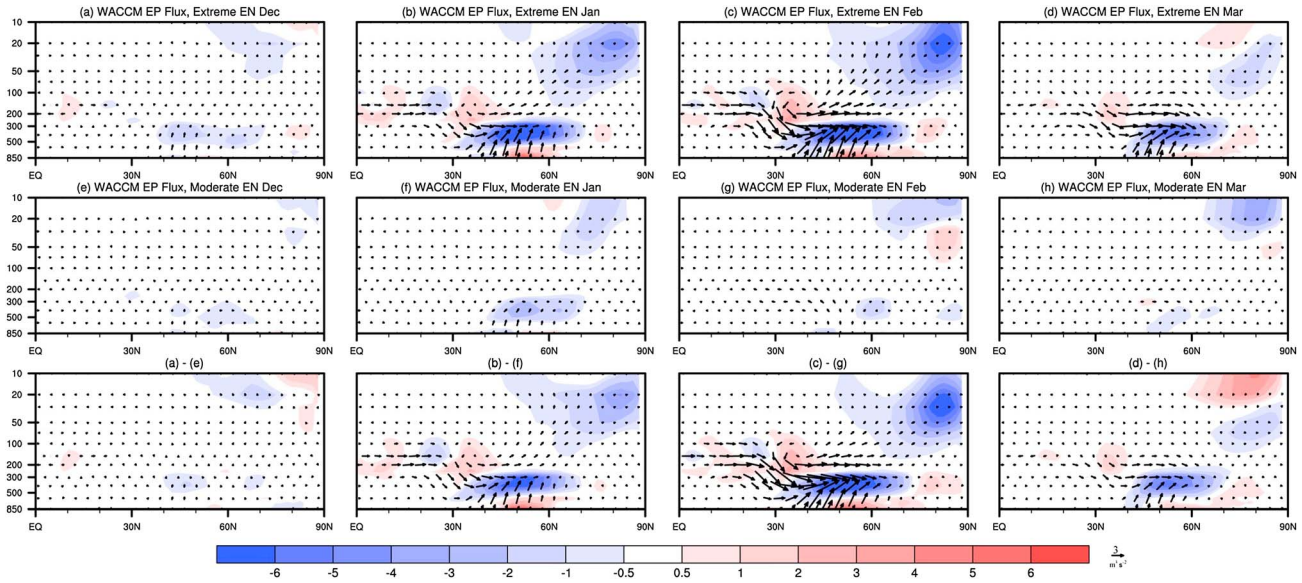

Figure 12. Response of the Eliassen-Palm (E-P) flux (vectors, normalized by air density; units: 10^7 m^3 s^{-2}) and the E-P flux divergence (color shading, units: m s^{-1} day^{-1}) from December to March, for (a–d) extreme El Niño (EN), (e–h) moderate El Niño, and (i–l) differences between them. The E-P flux is multiplied by the square root of 1,000/pressure (hPa) to better demonstrate the waves in the stratosphere.

to March, for extreme El Niño, moderate El Niño, and their differences. The anomalous upward propagation of planetary waves is well reproduced in both extreme and moderate El Niño cases. The anomalous upward component of the E-P flux, which is proportional to the meridional eddy heat flux, is dominant in the stratosphere between 40° and 60°N, leading to weakening of the northern polar vortex (Figures 10 and 11). Another common feature is that the wave activity develops from December when the SST forcing begins, peaks in February, and decays from March when the SST forcing is turned off. The evolution of wave activity is then responsible for the lagged response of the Arctic polar vortex (Figure 10). In addition, stronger upward wave activity is more excited by extreme El Niño than by moderate El Niño (Figures 12i–12l), accounting for a warmer stratosphere in the extreme El Niño case. Thus, the anomalous wave activity and subsequent stratospheric response associated with moderate and extreme El Niño show similar patterns but different amplitudes.

5. Summary and Discussion

The seasonal evolution of the response of the NH stratospheric vortex to extreme El Niño, compared with that to moderate El Niño, has been explored in observations derived from reanalysis data sets and simulations from WACCM4. Previous studies have found that it takes a few months for the stratosphere to establish a stable pattern of response to tropical SST anomalies (Calvo et al., 2004, 2010; Garcia-Herrera et al., 2006; Jin & Hoskins, 1995; Newman et al., 2001; Yulaeva & Wallace, 1994), and the lead-lag correlation analysis and simulations in our study further indicate that El Niño leads the stratospheric response by about 2 months. Although the composite polar vortex responses to extreme El Niño and moderate El Niño seem to be of opposite sign in winter (DJF), more careful analysis of individual El Niño events casts doubt on this result. Some events are not coherent with the composite results. We found little evidence for the opposite patterns of extreme and moderate El Niño. Also, it is not particularly surprising that the difference in response between extreme and moderate El Niño events is not statistically significant, due to the confounding effects of internal unforced variability. However, it was found that the patterns of circulation and temperature in late winter/early spring associated with extreme and moderate El Niño are similar, although the responses of extreme El Niño have larger amplitude than those of moderate El Niño.

Since the observational record is relatively short and internal climate variability can be large, the signatures of winter extreme and moderate El Niño were further confirmed by WACCM4 simulations. Simulations with SST forcing limited to winter (DJF) support the lagged response of the high-latitude stratosphere to El Niño.

Extreme El Niño has a clear impact on the NH polar stratospheric region in the form of an anomalous significant warming, similar to but with larger amplitude than that of moderate El Niño. Stronger upward propagation of planetary waves during extreme El Niño leads to a weaker Arctic polar vortex.

Recently, Rao and Ren (2016a, 2016b) have also analyzed the nonlinearity of the impacts of strong and moderate ENSO events on the NH stratosphere, reporting that the moderate El Niño is more efficient than the strong El Niño in modulating the extratropical circulation in winter. However, our study revealed a much stronger response of the NH stratospheric vortex (more than 4 times larger) to extreme El Niño than to moderate El Niño. The discrepancy may arise from the different methodologies we use, as we consider the lagged response of the stratosphere to winter El Niño; for example, we investigate the FMA-mean stratospheric circulation anomalies caused by DJF-mean El Niño events, while Rao and Ren (2016a, 2016b) analyzed the DJF-mean stratospheric circulation anomalies caused by DJF-mean El Niño events. The reason for considering the lagged response has already been illustrated in sections 3 and 4. Because the lagged response is considered here, the conclusions of the two studies are completely different. Moreover, this paper excludes CP El Niño events from the composites and only consider EP events, while Rao and Ren (2016a, 2016b) did not discriminate between the two types. The "strong" El Niño in their research is weaker than the extreme El Niño here. Specifically, the composite Niño3 peak of their strong events is 2.05 (Table 1 in Rao & Ren, 2016a), while ours is much larger at 2.99. To sum up, the contrasting conclusion, the consideration of the lagged response, and the different types of El Niño make our study different from Rao and Ren (2016a, 2016b, 2017).

Acknowledgments
We acknowledge the helpful suggestions and comments of two anonymous reviewers. This work was jointly supported by the SOA Program on Global Change and Air-Sea Interactions (GASI-IPOVAI-03), the National Natural Science Foundation of China (41575039 and 41530424), and the 973 Program (2014CB441202). We thank NCAR for providing the WACCM4 model (https://www2.cesm.ucar.edu/ models/current). The NCEPDOE Reanalysis was obtained from NOAA and is available at http://www.esrl.noaa.gov/psd/data/gridded/. The ERA-Interim reanalysis was obtained from http://apps.ecmwf.int/datasets/. The HadISST from the Met Office Hadley Centre is available at http://www.metoffice.gov.uk/hadobs/hadisst/data/download.html.

References

Andrews, D. G., Holton, J. R., & Leovy, C. B. (1987). *Middle atmosphere dynamics*. New York: Academic Press.

Ashok, K., Behera, S. K., Rao, S. A., Weng, H. Y., & Yamagata, T. (2007). El Niño Modoki and its possible teleconnection. *Journal of Geophysical Research*, *112*, C11007. https://doi.org/10.1029/2006JC003798

Avery, M. A., Davis, S. M., Rosenlof, K. H., Ye, H., & Dessler, A. E. (2017). Large anomalies in lower stratospheric water vapor and ice during the 2015–2016 El Niño. *Nature Geoscience*, *10*(6), 405–409. https://doi.org/10.1038/NGEO2961

Bjerknes, J. (1969). Atmospheric teleconnections from equatorial Pacific. *Monthly Weather Review*, *97*(3), 163–172. https://doi.org/10.1175/1520-0493(1969)097%3C0163:ATFTEP%3E2.3.CO;2

Brewer, A. (1949). Evidence for a world circulation provided by the measurements of helium and water vapour distribution in the stratosphere. *Quarterly Journal of the Royal Meteorological Society*, *75*(326), 351–363. https://doi.org/10.1002/qj.49707532603

Cagnazzo, C., Manzini, E., Calvo, N., Douglass, A., Akiyoshi, H., Bekki, S., et al. (2009). Northern winter stratospheric temperature and ozone responses to ENSO inferred from an ensemble of chemistry climate models. *Atmospheric Chemistry and Physics*, *9*(22), 8935–8948. https://doi.org/10.5194/acp-9-8935-2009

Cai, W., & Cowan, T. (2009). La Nina Modoki impacts Australia autumn rainfall variability. *Geophysical Research Letters*, *36*, L12805. https://doi.org/10.1029/2009GL037885

Cai, W. J., Borlace, S., Lengaigne, M., van Rensch, P., Collins, M., Vecchi, G., et al. (2014). Increasing frequency of extreme El Niño events due to greenhouse warming. *Nature Climate Change*, *4*(2), 111–116. https://doi.org/10.1038/Nclimate2100

Calvo, N., Garcia, R. R., Herrera, R. G., Puyol, D. G., Gimeno, L., Martin, E. H., & Rodriguez, P. R. (2004). Analysis of the ENSO signal in tropospheric and stratospheric temperatures observed by MSU, 1979–2000. *Journal of Climate*, *17*(20), 3934–3946.

Calvo, N., Garcia, R. R., Randel, W. J., & Marsh, D. R. (2010). Dynamical mechanism for the increase in tropical upwelling in the lowermost tropical stratosphere during warm ENSO events. *Journal of the Atmospheric Sciences*, *67*(7), 2331–2340. https://doi.org/10.1175/2010JAS3433.1

Calvo, N., Iza, M., Hurwitz, M. M., Manzini, E., Pena-Ortiz, C., Butler, A. H., et al. (2017). Northern Hemisphere Stratospheric Pathway of Different El Nino Flavors in Stratosphere-Resolving CMIP5 Models. *Journal of Climate*, *30*(12), 4351–4371. https://doi.org/10.1175/JCLI-D-16-0132.1

Camp, C. D., & Tung, K. K. (2007). Stratospheric polar warming by ENSO in winter: A statistical study. *Geophysical Research Letters*, *34*, L04809. https://doi.org/10.1029/2006GL028521

Changnon, S. A. (2000). *El Niño 1997–1998: The climate event of the century*. New York: Oxford University Press.

Chen, W., Takahashi, M., & Graf, H. F. (2003). Interannual variations of stationary planetary wave activity in the northern winter troposphere and stratosphere and their relations to NAM and SST. *Journal of Geophysical Research*, *108*(D24), 4797. https://doi.org/10.1029/2003JD003834

Chiodi, A. M., & Harrison, D. E. (2010). Characterizing warm-ENSO variability in the equatorial Pacific: An OLR perspective. *Journal of Climate*, *23*(9), 2428–2439. https://doi.org/10.1175/2009JCLI3030.1

Christiansen, B., Yang, S., & Madsen, M. S. (2016). Do strong warm ENSO events control the phase of the stratospheric QBO? *Geophysical Research Letters*, *43*, 10,489–10,495. https://doi.org/10.1002/2016GL070751

Dobson, G. (1956). Origin and distribution of the polyatomic molecules in the atmosphere. *Proceedings of the Royal Society of London. Series A: Mathematical and Physical Sciences*, *A236*(1205), 187–193.

Dobson, G. M., Harrison, D., & Lawrence, J. (1929). Measurements of the amount of ozone in the Earth's atmosphere and its relation to other geophysical conditions. Part III. *Proceedings of the Royal Society of London. Series A, Containing Papers of a Mathematical and Physical Character*, *122*(790), 456–486.

Domeisen, D. I. V., Butler, A. H., Frohlich, K., Bittner, M., Muller, W. A., & Baehr, J. (2015). Seasonal Predictability over Europe Arising from El Nino and Stratospheric Variability in the MPI-ESM Seasonal Prediction System. *Journal of Climate*, *28*(1), 256–271. https://doi.org/10.1175/Jcli-D-14-00207.1

Dunkerton, T. J. (2016). The quasi-biennial oscillation of 2015–2016: Hiccup or death spiral? *Geophysical Research Letters*, *43*, 10,547–10,552. https://doi.org/10.1002/2016GL070921

Edmon, H. J., Hoskins, B. J., & Mcintyre, M. E. (1980). Eliassen-Palm cross-sections for the troposphere. *Journal of the Atmospheric Sciences*, *37*(12), 2600–2616. https://doi.org/10.1175/1520-0469(1980)037%3C2600:EPCSFT%3E2.0.CO;2

Feng, J., & Li, J. P. (2011). Influence of El Niño Modoki on spring rainfall over south China. *Journal of Geophysical Research*, *116*, D13102. https://doi.org/10.1029/2010JD015160

Fletcher, C. G., & Kushner, P. J. (2011). The Role of Linear Interference in the Annular Mode Response to Tropical SST Forcing. *Journal of Climate*, *24*(3), 778–794. https://doi.org/10.1175/2010JCLI3735.1

Free, M., & Seidel, D. J. (2009). Observed El Niño–Southern Oscillation temperature signal in the stratosphere. *Journal of Geophysical Research*, *114*, D23108. https://doi.org/10.1029/2009JD012420

Fueglistaler, S., & Haynes, P. H. (2005). Control of interannual and longer-term variability of stratospheric water vapor. *Journal of Geophysical Research*, *110*, D24108. https://doi.org/10.1029/2005JD006019

Garcia, R. R., Marsh, D. R., Kinnison, D. E., Boville, B. A., & Sassi, F. (2007). Simulation of secular trends in the middle atmosphere, 1950–2003. *Journal of Geophysical Research*, *112*, D09301. https://doi.org/10.1029/2006JD007485

Garcia-Herrera, R., Calvo, N., Garcia, R. R., & Giorgetta, M. A. (2006). Propagation of ENSO temperature signals into the middle atmosphere: A comparison of two general circulation models and ERA-40 reanalysis data. *Journal of Geophysical Research*, *111*, D06101. https://doi.org/10.1029/2005JD006061

Garfinkel, C., Hurwitz, M., Waugh, D., & Butler, A. (2013). Are the teleconnections of central Pacific and eastern Pacific El Niño distinct in boreal wintertime? *Climate Dynamics*, *41*(7–8), 1835–1852. https://doi.org/10.1007/s00382-012-1570-2

Garfinkel, C. I., Gordon, A., Oman, L. D., Li, F., Davis, S., & Pawson, S. (2017). Nonlinear response of tropical lower stratospheric temperature and water vapor to ENSO. *Atmospheric Chemistry and Physics Discussions*, 1–35. https://doi.org/10.5194/acp-2017-520

Garfinkel, C. I., & Hartmann, D. L. (2007). Effects of the El Niño–Southern Oscillation and the quasi-biennial oscillation on polar temperatures in the stratosphere. *Journal of Geophysical Research*, *112*, D19112. https://doi.org/10.1029/2007JD008481

Garfinkel, C. I., & Hartmann, D. L. (2008). Different ENSO teleconnections and their effects on the stratospheric polar vortex. *Journal of Geophysical Research*, *113*, D18114. https://doi.org/10.1029/2008JD009920

Garfinkel, C. I., Hurwitz, M. M., Oman, L. D., & Waugh, D. W. (2013). Contrasting effects of central Pacific and eastern Pacific El Niño on stratospheric water vapor. *Geophysical Research Letters*, *40*, 4115–4120. https://doi.org/10.1002/grl.50677

Geller, M. A., Zhou, X. L., & Zhang, M. H. (2002). Simulations of the interannual variability of stratospheric water vapor. *Journal of the Atmospheric Sciences*, *59*(6), 1076–1085. https://doi.org/10.1175/1520-0469(2002)059%3C1076:SOTIVO%3E2.0.CO;2

Geng, X., Zhang, W. J., Stuecker, M. F., & Jin, F. F. (2017). Strong sub-seasonal wintertime cooling over East Asia and northern Europe associated with super El Nino events. *Scientific Reports*, *7*(1), 3770. https://doi.org/10.1038/S41598-017-03977-2

Gettelman, A., Randel, W. J., Massie, S., Wu, F., Read, W. G., & Russell, J. M. (2001). El Niño as a natural experiment for studying the tropical tropopause region. *Journal of Climate*, *14*(16), 3375–3392. https://doi.org/10.1175/1520-0442(2001)014%3C3375:ENOAAN%3E2.0.CO;2

Giese, B. S., & Ray, S. (2011). El Niño variability in simple ocean data assimilation (SODA), 1871–2008. *Journal of Geophysical Research*, *116*, C02024. https://doi.org/10.1029/2010JC006695

Graf, H. F., & Zanchettin, D. (2012). Central Pacific El Niño, the "subtropical bridge," and Eurasian climate. *Journal of Geophysical Research*, *117*, D01102. https://doi.org/10.1029/2011JD016493

Hamilton, K. (1993). An examination of observed Southern Oscillation effects in the Northern Hemisphere stratosphere. *Journal of the Atmospheric Sciences*, *50*(20), 3468–3474. https://doi.org/10.1175/1520-0469(1993)050%3C3468:AEOOSO%3E2.0.CO;2

Hamilton, K. (1995). Interannual variability in the Northern Hemisphere winter middle atmosphere in control and perturbed experiments with the GFDL SKYHI general circulation model. *Journal of the Atmospheric Sciences*, *52*(1), 44–66. https://doi.org/10.1175/1520-0469(1995)052%3C0044:IVITNH%3E2.0.CO;2

Hardiman, S. C., Butchart, N., Haynes, P. H., & Hare, S. H. E. (2007). A note on forced versus internal variability of the stratosphere. *Geophysical Research Letters*, *34*, L12803. https://doi.org/10.1029/2007GL029726

Hatsushika, H., & Yamazaki, K. (2003). Stratospheric drain over Indonesia and dehydration within the tropical tropopause layer diagnosed by air parcel trajectories. *Journal of Geophysical Research*, *108*(D19), 4610. https://doi.org/10.1029/2002JD002986

Hegyi, B. M., & Deng, Y. (2011). A dynamical fingerprint of tropical Pacific Sea surface temperatures on the decadal-scale variability of cool-season Arctic precipitation. *Journal of Geophysical Research*, *116*, D20121. https://doi.org/10.1029/2011JD016001

Horel, J. D., & Wallace, J. M. (1981). Planetary-scale atmospheric phenomena associated with the Southern Oscillation. *Monthly Weather Review*, *109*(4), 813–829. https://doi.org/10.1175/1520-0493(1981)109%3C0813:PSAPAW%3E2.0.CO;2

Hu, X., Yang, S., & Cai, M. (2016). Contrasting the eastern Pacific El Niño and the central Pacific El Niño: Process-based feedback attribution. *Climate Dynamics*, *47*(7-8), 2413–2424. https://doi.org/10.1007/s00382-015-2971-9

Hu, Y. Y., & Tung, K. K. (2002). Interannual and decadal variations of planetary wave activity, stratospheric cooling, and Northern Hemisphere annular mode. *Journal of Climate*, *15*(13), 1659–1673.

Hurrell, J. W., Holland, M. M., Gent, P. R., Ghan, S., Kay, J. E., Kushner, P. J., et al. (2013). The Community Earth System Model: A framework for collaborative research. *Bulletin of the American Meteorological Society*, *94*(9), 1339–1360. https://doi.org/10.1175/Bams-D-12-00121.1

Hurwitz, M. M., Calvo, N., Garfinkel, C. I., Butler, A. H., Ineson, S., Cagnazzo, C., et al. (2014). Extra-tropical atmospheric response to ENSO in the CMIP5 models. *Climate Dynamics*, *43*(12), 3367–3376. https://doi.org/10.1007/s00382-014-2110-z

Hurwitz, M. M., Newman, P. A., Oman, L. D., & Molod, A. M. (2011). Response of the Antarctic stratosphere to two types of El Niño events. *Journal of the Atmospheric Sciences*, *68*(4), 812–822. https://doi.org/10.1175/2011JAS3606.1

Hurwitz, M. M., Song, I.-S., Oman, L. D., Newman, P. A., Molod, A. M., Frith, S. M., & Nielsen, J. E. (2011). Response of the Antarctic stratosphere to warm pool El Niño events in the GEOS CCM. *Atmospheric Chemistry and Physics*, *11*(18), 9659–9669. https://doi.org/10.5194/acp-11-9659-2011

Ineson, S., & Scaife, A. A. (2009). The role of the stratosphere in the European climate response to El Nino. *Nature Geoscience*, *2*(1), 32–36. https://doi.org/10.1038/NGEO381

Iza, M., & Calvo, N. (2015). Role of stratospheric sudden warmings on the response to central Pacific El Niño. *Geophysical Research Letters*, *42*, 2482–2489. https://doi.org/10.1002/2014GL062935

Iza, M., Calvo, N., & Manzini, E. (2016). The stratospheric pathway of La Nina. *Journal of Climate*, *29*(24), 8899–8914. https://doi.org/10.1175/JCLI-D-16-0230.1

Jin, F.-F., & Hoskins, B. J. (1995). The direct response to tropical heating in a baroclinic atmosphere. *Journal of the Atmospheric Sciences*, *52*(3), 307–319. https://doi.org/10.1175/1520-0469(1995)052%3C0307:TDRTTH%3E2.0.CO;2

Kao, H. Y., & Yu, J. Y. (2009). Contrasting eastern-Pacific and central-Pacific types of ENSO. *Journal of Climate*, *22*(3), 615–632. https://doi.org/10.1175/2008JCLI2309.1

Kug, J.-S., Choi, J., An, S.-I., Jin, F.-F., & Wittenberg, A. T. (2010). Warm pool and cold tongue El Niño events as simulated by the GFDL 2.1 coupled GCM. *Journal of Climate*, *23*(5), 1226–1239. https://doi.org/10.1175/2009JCLI3293.1

Kug, J.-S., Jin, F.-F., & An, S.-I. (2009). Two types of El Niño events: Cold tongue El Niño and warm pool El Niño. *Journal of Climate*, *22*(6), 1499–1515. https://doi.org/10.1175/2008JCLI2624.1

Labitzke, K., Kunzel, M., & Bronnimann, S. (2006). Sunspots, the QBO and the stratosphere in the North Polar region—20 years later. *Meteorologische Zeitschrift*, *15*(3), 355–363. https://doi.org/10.1127/0941-2948/2006/0136

Labitzke, K., & Loon, H. (1989). The Southern Oscillation. Part IX: The influence of volcanic eruptions on the Southern Oscillation in the stratosphere. *Journal of Climate*, *2*(10), 1223–1226. https://doi.org/10.1175/1520-0442(1989)002%3C1223:TSOPIT%3E2.0.CO;2

Lan, X. Q., Chen, W., & Wang, L. (2012). Quasi-stationary planetary wave-mean flow interactions in the Northern Hemisphere stratosphere and their responses to ENSO events. *Science China: Earth Sciences*, *55*(3), 405–417. https://doi.org/10.1007/S11430-011-4345-4

Larkin, N. K., & Harrison, D. E. (2005a). Global seasonal temperature and precipitation anomalies during El Niño autumn and winter. *Geophysical Research Letters*, *32*, L16705. https://doi.org/10.1029/2005GL022860

Larkin, N. K., & Harrison, D. E. (2005b). On the definition of El Niño and associated seasonal average US weather anomalies. *Geophysical Research Letters*, *32*, L13705. https://doi.org/10.1029/2005GL022738

Levine, A. F. Z., & McPhaden, A. J. (2016). How the July 2014 easterly wind burst gave the 2015–2016 El Niño a head start. *Geophysical Research Letters*, *43*, 6503–6510. https://doi.org/10.1002/2016GL069204

L'Heureux, M. L., Takahashi, K., Watkins, A. B., Barnston, A. G., Becker, E. J., Di Liberto, T. E., et al. (2017). Observing and predicting the 2015/16 El Nino. *Bulletin of the American Meteorological Society*, *98*(7), 1363–1382. https://doi.org/10.1175/BAMS-D-16-0009.1

Li, J. P., Sun, C., & Jin, F.-F. (2013). NAO implicated as a predictor of Northern Hemisphere mean temperature multidecadal variability. *Geophysical Research Letters*, *40*, 5497–5502. https://doi.org/10.1002/2013GL057877

Li, Y., Li, J. P., Zhang, W. J., Chen, Q. L., Feng, J., Zheng, F., et al. (2017). Impacts of the tropical Pacific cold tongue mode on ENSO diversity under global warming. *Journal of Geophysical Research: Oceans*, *122*, 8524–8542. https://doi.org/10.1002/2017JC013052

Li, Y., Li, J. P., Zhang, W. J., Zhao, X., Xie, F., & Zheng, F. (2015). Ocean dynamical processes associated with the tropical Pacific cold tongue mode. *Journal of Geophysical Research: Oceans*, *120*, 6419–6435. https://doi.org/10.1002/2015JC010814

Manzini, E., Giorgetta, M. A., Esch, M., Kornblueh, L., & Roeckner, E. (2006). The influence of sea surface temperatures on the northern winter stratosphere: Ensemble simulations with the MAECHAM5 model. *Journal of Climate*, *19*(16), 3863–3881. https://doi.org/10.1175/Jcli3826.1

Marsh, D. R., Mills, M. J., Kinnison, D. E., Lamarque, J. F., Calvo, N., & Polvani, L. M. (2013). Climate change from 1850 to 2005 simulated in CESM1 (WACCM). *Journal of Climate*, *26*(19), 7372–7391. https://doi.org/10.1175/JCLI-D-12-00558.1

Matthes, K., Langematz, U., Gray, L. L., Kodera, K., & Labitzke, K. (2004). Improved 11-year solar signal in the freie universitat Berlin climate middle atmosphere model (FUB-CMAM). *Journal of Geophysical Research*, *109*, D06101. https://doi.org/10.1029/2003JD004012

Matthewman, N. J., & Esler, J. G. (2011). Stratospheric sudden warmings as self-tuning resonances. Part I: Vortex splitting events. *Journal of the Atmospheric Sciences*, *68*(11), 2481–2504. https://doi.org/10.1175/Jas-D-11-07.1

McPhaden, M. J. (1999). El Niño: The child prodigy of 1997–98. *Nature*, *398*(6728), 559–561. https://doi.org/10.1038/19193

McPhaden, M. J., Zebiak, S. E., & Glantz, M. H. (2006). ENSO as an integrating concept in Earth science. *Science*, *314*(5806), 1740–1745. https://doi.org/10.1126/science.1132588

Mitchell, D. M., Gray, L. J., & Charlton-Perez, A. J. (2011). The structure and evolution of the stratospheric vortex in response to natural forcings. *Journal of Geophysical Research*, *116*, D15110. https://doi.org/10.1029/2011JD015788

Mukougawa, H., & Hirooka, T. (2004). Predictability of stratospheric sudden warming: A case study for 1998/99 winter. *Monthly Weather Review*, *132*(7), 1764–1776. https://doi.org/10.1175/1520-0493(2004)132%3C1764:POSSWA%3E2.0.CO;2

Newman, P. A., Nash, E. R., & Rosenfield, J. E. (2001). What controls the temperature of the Arctic stratosphere during the spring? *Journal of Geophysical Research*, *106*, 19,999–20,010. https://doi.org/10.1029/2000JD000061

Noguchi, S., Mukougawa, H., Kuroda, Y., Mizuta, R., Yabu, S., & Yoshimura, H. (2016). Predictability of the stratospheric polar vortex breakdown: An ensemble reforecast experiment for the splitting event in January 2009. *Journal of Geophysical Research: Atmospheres*, *121*, 3388–3404. https://doi.org/10.1002/2015JD024581

Palmeiro, F., Iza, M., Barriopedro, D., Calvo, N., & Garcia-Herrera, R. (2017). The complex behavior of El Niño winter 2015–2016. *Geophysical Research Letters*, *44*, 2902–2910. https://doi.org/10.1002/2017GL072920

Philander, S. G. H. (1983). Anomalous El Niño of 1982–83. *Nature*, *305*(5929), 16. https://doi.org/10.1038/305016a0

Pyper, B. J., & Peterman, R. M. (1998). Comparison of methods to account for autocorrelation in correlation analyses of fish data. *Canadian Journal of Fisheries and Aquatic Sciences*, *55*(9), 2127–2140. https://doi.org/10.1139/f98-104

Randel, W. J. (1987). A study of planetary-waves in the southern winter troposphere and stratosphere. Part 1: Wave structure and vertical propagation. *Journal of the Atmospheric Sciences*, *44*(6), 917–935. https://doi.org/10.1175/1520-0469(1987)044%3C0917:ASOPWI%3E2.0.CO;2

Randel, W. J., Garcia, R. R., Calvo, N., & Marsh, D. (2009). ENSO influence on zonal mean temperature and ozone in the tropical lower stratosphere. *Geophysical Research Letters*, *36*, L15822. https://doi.org/10.1029/2009GL039343

Rao, J., & Ren, R. (2015). A decomposition of ENSO's impacts on the northern winter stratosphere: Competing effect of SST forcing in the tropical Indian Ocean. *Climate Dynamics*, *46*(11-12), 3689–3707. https://doi.org/10.1007/s00382-015-2797-5

Rao, J., & Ren, R. C. (2016a). Asymmetry and nonlinearity of the influence of ENSO on the northern winter stratosphere: 1. Observations. *Journal of Geophysical Research: Atmospheres*, *121*, 9000–9016. https://doi.org/10.1002/2015JD024520

Rao, J., & Ren, R. C. (2016b). Asymmetry and nonlinearity of the influence of ENSO on the northern winter stratosphere: 2. Model study with WACCM. *Journal of Geophysical Research: Atmospheres*, *121*, 9017–9032. https://doi.org/10.1002/2015JD024521

Rao, J., & Ren, R. C. (2017). Parallel comparison of the 1982/83, 1997/98 and 2015/16 super El Ninos and their effects on the extratropical stratosphere. *Advances in Atmospheric Sciences*, *34*(9), 1121–1133. https://doi.org/10.1007/s00376-017-6260-x

Rayner, N. A., Parker, D. E., Horton, E. B., Folland, C. K., Alexander, L. V., Rowell, D. P., et al. (2003). Global analyses of sea surface temperature, sea ice, and night marine air temperature since the late nineteenth century. *Journal of Geophysical Research*, *108*(D14), 4407. https://doi.org/10.1029/2002JD002670

Ren, H. L., & Jin, F. F. (2011). Niño indices for two types of ENSO. *Geophysical Research Letters*, *38*, L04704. https://doi.org/10.1029/2010GL046031

Ren, R. C., Cai, M., Xiang, C. Y., & Wu, G. X. (2012). Observational evidence of the delayed response of stratospheric polar vortex variability to ENSO SST anomalies. *Climate Dynamics*, *38*(7–8), 1345–1358. https://doi.org/10.1007/s00382-011-1137-7

Richter, J. H., Deser, C., & Sun, L. (2015). Effects of stratospheric variability on El Nino teleconnections. *Environmental Research Letters*, *10*(12). https://doi.org/10.1088/1748-9326/10/12/124021

Sassi, F., Kinnison, D., Boville, B. A., Garcia, R. R., & Roble, R. (2004). Effect of El Niño–Southern Oscillation on the dynamical, thermal, and chemical structure of the middle atmosphere. *Journal of Geophysical Research*, *109*, D17108. https://doi.org/10.1029/2003JD004434

Scaife, A. A., Butchart, N., Jackson, D. R., & Swinbank, R. (2003). Can changes in ENSO activity help to explain increasing stratospheric water vapor? *Geophysical Research Letters*, *30*(17), 1880. https://doi.org/10.1029/2003GL017591

Schar, C., Ban, N., Fischer, E. M., Rajczak, J., Schmidli, J., Frei, C., et al. (2016). Percentile indices for assessing changes in heavy precipitation events. *Climatic Change*, *137*(1–2), 201–216. https://doi.org/10.1007/s10584-016-1669-2

Shinoda, T., Hurlburt, H. E., & Metzger, E. J. (2011). Anomalous tropical ocean circulation associated with La Nina Modoki. *Journal of Geophysical Research*, *116*, C12001. https://doi.org/10.1029/2011JC007304

Sigmond, M., Scinocca, J. F., Kharin, V. V., & Shepherd, T. G. (2013). Enhanced seasonal forecast skill following stratospheric sudden warmings. *Nature Geoscience*, *6*(2), 98–102. https://doi.org/10.1038/NGEO1698

Simmons, A., Uppala, S., & Dee, D. (2007). Update on ERA-Interim. *ECMWF Newsletter*, *111*(5).

Simmons, A., Uppala, S., Dee, D., & Kobayashi, S. (2007). ERA-Interim: New ECMWF reanalysis products from 1989 onwards. *ECMWF Newsletter*, *110*(110), 25–35.

Singh, A., Delcroix, T., & Cravatte, S. (2011). Contrasting the flavors of El Niño–Southern Oscillation using sea surface salinity observations. *Journal of Geophysical Research*, *116*, C06016. https://doi.org/10.1029/2010JC006862

Solomon, S., Kinnison, D., Bandoro, J., & Garcia, R. (2015). Simulation of polar ozone depletion: An update. *Journal of Geophysical Research: Atmospheres*, *120*, 7958–7974. https://doi.org/10.1002/2015JD023365

Sung, M. K., Kim, B. M., & An, S. I. (2014). Altered atmospheric responses to eastern Pacific and central Pacific El Niños over the North Atlantic region due to stratospheric interference. *Climate Dynamics*, *42*(1–2), 159–170. https://doi.org/10.1007/s00382-012-1661-0

Taguchi, M., & Hartmann, D. L. (2006). Increased occurrence of stratospheric sudden warmings during El Niño as simulated by WACCM. *Journal of Climate*, *19*(3), 324–332. https://doi.org/10.1175/JCLI3655.1

Trenberth, K. E., Branstator, G. W., Karoly, D., Kumar, A., Lau, N. C., & Ropelewski, C. (1998). Progress during TOGA in understanding and modeling global teleconnections associated with tropical sea surface temperatures. *Journal of Geophysical Research*, *103*, 14,291–14,324. https://doi.org/10.1029/97JC01444

Trenberth, K. E., & Stepaniak, D. P. (2001). Indices of El Nino evolution. *Journal of Climate*, *14*(8), 1697–1701.

Uppala, S., Dee, D., Kobayashi, S., Berrisford, P., & Simmons, A. (2008). Towards a climate data assimilation system: Status update of ERA-Interim. *ECMWF Newsletter*, *115*(7), 12–18.

Van Loon, H., & Labitzke, K. (1987). The Southern Oscillation. 5. The anomalies in the lower stratosphere of the Northern Hemisphere in winter and a comparison with the quasi-biennial oscillation. *Monthly Weather Review*, *115*(2), 357–369. https://doi.org/10.1175/1520-0493(1987)115%3C0357:TSOPVT%3E2.0.CO;2

Van Loon, H., Zerefos, C., & Repapis, C. (1982). The Southern Oscillation in the stratosphere. *Monthly Weather Review*, *110*(3), 225–229. https://doi.org/10.1175/1520-0493(1982)110%3C0225:TSOITS%3E2.0.CO;2

Varotsos, C. A., Sarlis, N. V., & Efstathiou, M. (2017). On the association between the recent episode of the quasi-biennial oscillation and the strong El Niño event. *Theoretical and Applied Climatology*. https://doi.org/10.1007/s00704-017-2191-9

Wang, G., Cai, W., Gan, B., Wu, L., Santoso, A., Lin, X., et al. (2017). Continued increase El Niño frequency long after 1.5 warming stabilization. *Nature Climate Change*, *7*(8), 568–572. https://doi.org/10.1038/NCLIMATE3351

Wei, K., Chen, W., & Huang, R. H. (2007). Association of tropical Pacific Sea surface temperatures with the stratospheric Holton-Tan oscillation in the Northern Hemisphere winter. *Geophysical Research Letters*, *34*, L16814. https://doi.org/10.1029/2007GL030478

Weng, H. Y., Ashok, K., Behera, S. K., Rao, S. A., & Yamagata, T. (2007). Impacts of recent El Niño Modoki on dry/wet conditions in the Pacific rim during boreal summer. *Climate Dynamics*, *29*(2–3), 113–129. https://doi.org/10.1007/s00382-007-0234-0

WMO (World Meteorological Organization) (2003). Scientific Assessment of Ozone depletion: 2002. In *Global Ozone Research and Monitoring Project* (Report No. 47, 498 pp.). Geneva.

Xie, F., Li, J., Tian, W., Feng, J., & Huo, Y. (2012). Signals of El Niño Modoki in the tropical tropopause layer and stratosphere. *Atmospheric Chemistry and Physics*, *12*(11), 5259–5273. https://doi.org/10.5194/acp-12-5259-2012

Xie, F., Li, J. P., Tian, W. S., Zhang, J. K., & Shu, J. C. (2014). The impacts of two types of El Niño on global ozone variations in the last three decades. *Advances in Atmospheric Sciences*, *31*(5), 1113–1126. https://doi.org/10.1007/s00376-013-3166-0

Xie, F., Li, J. P., Tian, W. S., Zhang, J. K., & Sun, C. (2014). The relative impacts of El Niño Modoki, canonical El Niño, and QBO on tropical ozone changes since the 1980s. *Environmental Research Letters*, *9*(6), 064020. https://doi.org/10.1088/1748-9326/9/6/064020

Xie, F., Tian, W., Austin, J., Li, J., Tian, H., Shu, J., & Chen, C. (2011). The effect of ENSO activity on lower stratospheric water vapor. *Atmospheric Chemistry and Physics Discussions*, *11*(2), 4141–4166. https://doi.org/10.5194/acpd-11-4141-2011

Xu, G. Z., Osborn, T. J., Matthews, A. J., & Joshi, M. M. (2016). Different atmospheric moisture divergence responses to extreme and moderate El Ninos. *Climate Dynamics*, *47*(1–2), 393–410. https://doi.org/10.1007/s00382-015-2844-2

Yeh, S. W., Kirtman, B. P., Kug, J. S., Park, W., & Latif, M. (2011). Natural variability of the central Pacific El Niño event on multi-centennial timescales. *Geophysical Research Letters*, *38*, L02704. https://doi.org/10.1029/2011GL045886

Yeh, S.-W., Kug, J.-S., Dewitte, B., Kwon, M.-H., Kirtman, B. P., & Jin, F.-F. (2009). El Niño in a changing climate. *Nature*, *461*(7263), 511–514. https://doi.org/10.1038/nature08316

Yoden, S. (1987). Bifurcation properties of a stratospheric vacillation model. *Journal of the Atmospheric Sciences*, *44*(13), 1723–1733. https://doi.org/10.1175/1520-0469(1987)044%3C1723:BPOASV%3E2.0.CO;2

Yulaeva, E., & Wallace, J. M. (1994). The signature of ENSO in global temperature and precipitation fields derived from the microwave sounding unit. *Journal of Climate*, *7*(11), 1719–1736. https://doi.org/10.1175/1520-0442(1994)007%3C1719:TSOEIG%3E2.0.CO;2

Zhang, W. J., Jin, F. F., Li, J. P., & Ren, H. L. (2011). Contrasting impacts of two-type El Niño over the western North Pacific during boreal autumn. *Journal of the Meteorological Society of Japan*, *89*(5), 563–569. https://doi.org/10.2151/jmsj.2011-510

Zhang, W. J., Jin, F. F., & Turner, A. (2014). Increasing autumn drought over southern China associated with ENSO regime shift. *Geophysical Research Letters*, *41*, 4020–4026. https://doi.org/10.1002/2014GL060130

Zhang, W. J., Jin, F. F., Zhao, J. X., Qi, L., & Ren, H. L. (2013). The possible influence of a nonconventional El Niño on the severe autumn drought of 2009 in southwest China. *Journal of Climate*, *26*(21), 8392–8405. https://doi.org/10.1175/JCLI-D-12-00851.1

Zhang, W. J., Wang, L., Xiang, B. Q., Qi, L., & He, J. H. (2015). Impacts of two types of La Nina on the NAO during boreal winter. *Climate Dynamics*, *44*(5–6), 1351–1366. https://doi.org/10.1007/s00382-014-2155-z

Zubiaurre, I., & Calvo, N. (2012). The El Niño–Southern Oscillation (ENSO) Modoki signal in the stratosphere. *Journal of Geophysical Research*, *117*, D04104. https://doi.org/10.1029/2011JD016690